Mechanics & Industry **17**, 105 (2016)
© AFM, EDP Sciences 2015
DOI: 10.1051/meca/2015050
www.mechanics-industry.org

Mechanics & Industry

Modeling and experimental verification of a 25W fabricated PEM fuel cell by parametric and GMDH-type neural network

Seyed Mohsen Pourkiaei[1], Mohammad Hossein Ahmadi[2,a] and S. Mahmoud Hasheminejad[1]

[1] Department of Energy, Material and Energy Research Center, Karaj, Iran
[2] Department of Mechanical Engineering, Pardis Branch, Islamic Azad University, Pardis New City, Tehran, Iran

Received 29 November 2014, Accepted 19 June 2015

Abstract – In this paper two artificial intelligence techniques to predict and control behavior of a 25W fabricated proton exchange membrane (PEM) fuel cell, have been investigated. These approaches are: "Parametric Neural Network (PNN)" and "Group Method of Data Handling (GMDH)" for the first time. A PNN model is developed by introducing a "*p*" parameter in the activation function of the neural network. PNN model with its specific tangent hyperbolic transfer function have the ability to be with different nonlinearity degrees of input data. To develop GMDH network, quadratic polynomial was utilized. To determine proper weights of GMDH network, back propagation algorithm has been used. The input layer consists of gas pressure, fuel cell temperature and input current experimental data, to predict the output voltage. The results show that both generalized Parametric and GMDH-type neural networks are reliable tools to predict the output voltage of PEM fuel cell with high coefficient of determination values of 0.96 and 0.98.

Key words: Proton exchange membrane fuel cell / hydrogen modeling / output voltage prediction / parametric neural network / group method of data handling

1 Introduction

Proton exchange membrane fuel cells (PEMFCs) have a great potential for fossil fuel power sources replacement due to the decrease of petroleum based energy resources, increasing power demand, rising of the oil prices and global warming. Fuel cell technologies have received much attention in recent years owing to their advantages such as higher efficiency, no dependence on fossil fuels, no emissions of polluting and greenhouse gases (SOx, NOx, CO_2, CO) and silent performance due to no mobile parts and, etc. Fuel cells, which are classified by their electrolyte type, are electrochemical devices that convert chemical energy stored in fuels such as hydrogen to electrical energy directly, without combustion process. Their efficiency can reach as high as 60% in electrical energy conversion and overall 80% in combined heat and power (CHP) systems, with >90% reduction in major pollutants [1, 2]. Among different types of fuel cells, PEMFC due to low operating pressure and temperature and high power density is more suitable than other types of fuel cell for vehicles and local hydrogen production purposes. Their optimum operating temperature is below 90 °C. As an outline, reactions in a PEM fuel cell can be illustrated as following: hydrogen in anode electrode changes into hydrogen ions, and electrons are released. The membrane just let the ions to pass through, so electrons move through an external circuit creating the electric current. The ions reaching the cathode are reduced with the electrons and oxygen, and finally water is a byproduct. Redox reactions are shown as below:

Reaction at anode:

$$H_2 \rightarrow 2H^+ + 2e \quad (1)$$

Reaction at cathode:

$$1/2\ O_2 + 2e + 2H^+ \rightarrow H_2O \quad (2)$$

PEM fuel cells considerable features such as low operating temperature, high power density, rapid load change compatibility and easy assembling, have made them a reliable choice for the next generation power sources for transportation, stationary, and portable applications [3–12]. We require a suitable predicting model to have a correct and comprehensive view of a fuel cell before the operation, determination of the optimal operating conditions and also checking the operation conditions that cannot be tested or measured. The purpose of this study is to

[a] Corresponding author: mohammadhosein.ahmadi@gmail.com

Nomenclature

Symbols	
P	Pressure (Bar)
T	Temperature (°C)
I	Current (A)
V	Output voltage (V)
V_C	Cell voltage (V)
P_e	Electric power (W)
n	Number of cells
F	Faraday constant
N	Total number of training output
O_j	Output of jth layer
y_i	Predicted output
$\hat{y}_i$	Real output value
$\bar{y}_i$	Mean of predicted output
E	Mean squares error function
x	Input
b_j	Bias
f_p	Parametric transfer function
t	Target (real output)
O_o	Network output
x_h	Output signal of weights of first hidden layer
x_o	Output signal of weights of second hidden layer
p	Parametric neural network regulator
O_h	Output of first hidden layer
Greek	
β	Learning rate
α	Momentum factor
$g(t)$	Gradient of SSE
σ	Slope of transfer function
δ_{o_o}	Returned signal from output to second hidden layer
δ_{o_i}	Returned signal from second hidden layer
δ_{h_o}	Returned signal from second hidden layer weights
δ_{h_i}	Returned signal from first hidden layer
Terminology	
SSE	Sum of square error
MAPE Mean	Absolute percentage error

achieve this kind of model by the neural network. In general, modeling for the fuel cells can be divided into two categories: theoretical models based on mass and energy conservation laws and physical relations of mass, momentum and heat; and semi-empirical models based on numerical calculations and data obtained from experimental tests. Several models have been proposed for the control of fuel cell systems in which, various simplifications, software and boundary conditions are used. Semi-empirical methods present an efficient model from experimentally derived data that can model the effects of changing parameters. Relative humidity, reactant gas stoichiometry, gases pressures and temperature are just some of the parameters which are involved in PEM fuel cells process. Many articles are available on the steady-state models, mainly focused on the design of the PEM fuel cell and select its optimal function point [13]. Baschuk and Li presented an integrated physical and electrochemical model for various cells components [14]. Nguyen and White developed a model to evaluate different humidities [15]. The model accounts for water transport across the membrane by electro-osmosis and diffusion, heat transfer from the solid phase to the gas phase and latent heat associated with water evaporation and condensation in the flow channels. Fuller and Newman simulated PEM fuel cell operation in different electrodes feed statuses of wet gas [16]. Water management, thermal management, and fuel consumption were examined in detail. Bernardi and Verbrugge presented a simple one-dimensional mathematical model for water transport in porous electrodes [17]. They also investigated the factors that limit cell performance. Wang et al investigated flow and two-phase transmission of gas-liquid in a PEM fuel cell (anode air) and also, methanol fuel cell [18]. Du and Shi have provided a Computational fluid dynamics (CFD) model for the dense structured catalyst layer [19]. In fact, relatively few

models have been presented in the literature for transient behavior and control of fuel cell systems [20]. With a Quasi-three dimensional dynamic model for a PEM fuel cell by Mueller et al. [21], that dynamic equations were solved for a typical but simplified quasi-three dimensional geometric representation of a single cell repeat unit of a fuel cell stack. A model for predicting cell loads, with emphasis on the response time to change the dynamics of the system temperature was proposed by Shan and Choe [22]. Simulations had been performed to analyze the effects of load currents on the behaviors of the fuel cell. A control strategy based forward-looking model was studied by Na et al. [23]. A linearization approach to generate a dynamic model is presented by Nasiri [24]. The mentioned static and dynamic models, built the basic foundation for the study of mechanisms and understanding of the physical phenomena in polymer fuel cells. Despite advances in the modeling, physical models proposed for fuel cells are not sufficiently accurate due to complex nonlinear nature of their process. Usually modeling is performed by providing models that are based on knowledge of the chemical and physical phenomena. These models require a good understanding of their process parameters. In many cases, determining the parameters for operating a fuel cell system is difficult [25]. One way to solve this problem is the exploitation of raw experimental data with a "black box" model that requires no initial knowledge about the system. Several techniques can be used to create a black-box model, however, a neural network model that is well designed, provides a functional and accurate input-output relationship that is due to its excellent ability to multi-dimensional topography. Neural network can predict the desired output variables faster and more accurate than doing a physical model. For this reason, it is widely used in various fields of science and technology. Most neural network models presented in papers have been investigated for fuel cell systems from active and dynamic aspects. Ogaji et al. [26] presented a Multi-Layer Perceptron (MLP) neural network with cell temperature and pressure input and output voltage. Ou and Achenie [27] presented a hybrid neural network model to evaluate the effect of Pt loading. Chávez-Ramírez [28] developed a neural network model for high power PEM fuel cell [28]. Sisworahardjo [29] investigated a feed forward neural network model for a 100 W portable fuel cell with input parameters of current and temperature to estimate hydrogen flow rate and voltage. In reference [30] the author developed an optimal model for PEM fuel cell, based on Taguchi method using neural networks and genetic algorithms. A neural network-based model for the dynamic mechanical behavior of a PEM fuel cell is presented in reference [31]. The associated experimental conditions specifying the vibration tests to train and validate were defined. Kim and Lee [32] checked the diagnosis and health status of PEM fuel cell using output voltage algorithm and Hamming Neural Network (HNN). In this paper, a specific transfer functioned neural network which we named "parametric neural network" is designed to predict behavior of a fabricated 25W PEM fuel cell. The input layer consists of gas pressure, current and temperature and the output layer consists of voltage. A number of studies has been done in GMDH method and NN for engineering fields. System classification techniques are employed in different fields to model and predict the performance of unknown and complicated systems based on given input-output data [33]. For this reason, soft computing methods, which involve computation in an imprecise environment, have attracted considerable attention of researchers. The components of fuzzy logic, neural network and evolutionary algorithms have great potential in solving complex non-linear system classification and control problems [34]. Many studies have been done to use evolutionary methods as suitable tools for system classification [35–37]. Among these methods, the group method of data handling (GMDH) algorithm is a self-organizing method which is generated based on the evaluation of their performances on a set of multi-input and single output data pairs $(\mathrm{X}i, \mathrm{Y}i)$ $(i = 1, 2, \ldots, M)$. The GMDH was investigated by Ivakhnenko [38] as a multivariable analysis approach for complex systems modeling and classification. In this way, the GMDH can be employed to model complicated systems without having exact knowledge of the systems. The GMDH works by creating an analytical function in a feed forward network based on a quadratic node transfer function in which coefficients are achieved by regression process [39]. Actually, the real GMDH algorithm in which the model coefficients are approximated by means of the least square method has been categorized as complete induction and incomplete induction, which represent the combinatorial (COMBI) and multi-layered iterative algorithms (MIA), respectively [40]. Use of self-organizing networks has result in successful application of the GMDH type algorithm in a wide range of engineering, science and economics [41–47]. A comprehensive review of utilizing evolutionary algorithms in the design of artificial neural networks is presented in reference [48]. In recent years, genetic algorithms have been used in a feed forward GMDH type neural network for each neuron searching its best set of connection with the preceding layer [49]. In the present work, models are developed with respect to GMDH and ANN and experimental PEM fuel cell. The results are verified against experimental values. The paper is organized as follows: Fabricated fuel cell system and experimental steps are reported in the next section. Section 3 provides different steps to develop the parametric ANN-based models. Results and discussions are reported in Section 4.

2 Fabricated PEM fuel cell system and experimental steps

2.1 Fabricated PEM fuel cell

In line with this project, to provide training data for the neural network, a PEM fuel cell was needed. In order to eliminate this need, a PEM fuel cell was designed and built commensurate with the project. After designing the

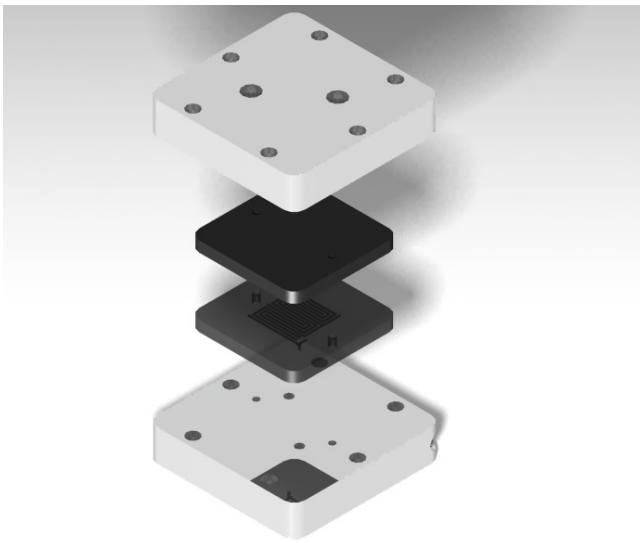

Fig. 1. Three-dimensional view of end plates and graphite electrodes design.

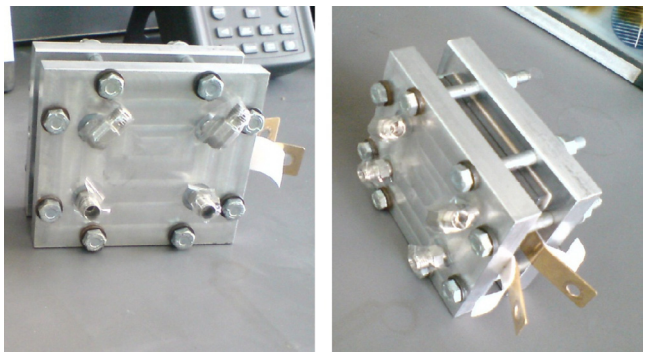

Fig. 2. Final fabricated PEM fuel cell.

components, the fuel cell was built and assembled in Material and research center of Isfahan. The fabricated PEM is a double cell stack, with 25 cm^2 active area for each cell. The membrane current density is 0.8–1 A/cm^2. The fabricated PEM is a Hydrogen-Oxygen type and therefore the catalyst for both anode and cathode electrodes sides was the same and made of carbon-platinum. The catalyst load is 0.5 gr/cm^2. Depth of the graphite electrodes gas transmission channels is considered 1 mm. Figure 1 shows a three-dimensional view of end plates and graphite electrodes design. The final fabricated PEM fuel cell is depicted in Figure 2.

2.2 Experimental tests

There were some operational preconditions that should be respected for the fuel cell tests. To perform the tests on the fabricated PEM fuel cell the following points were required to be observed:

- Humidity of 95% is required in the input gas. The definition of the humidity is the ratio of the partial pressure of water vapor in an air-water mixture to the saturated vapor pressure of water at a prescribed temperature or relative humidity of the exhaust gas.
- Pressure difference between two sides of the membrane should not be over −0.5 bar.
- The maximum acceptable operating pressure for the inlet gas is 2 bar.
- To begin the test, the open circuit voltage should be reached to 1.9 V.
- The acceptable stoichiometric ratio of the reaction is 1 or 1.5 for both the anode and cathode side.
- During the test, cell voltage should not reach to less than 0.4 V, because in that case due to the high current density, fuel does not reach the catalyst sites and called catalyst starvation occurs.

For running the fuel cell for the first time the break in process is needed. The break in process is necessary to have a stable performance and also prevention of thermal shocks and possible leaks in the system. This operation is performed by injection of the moist inert gas, such as N_2, to the fuel cell and the increasing cell temperature with increasing the inlet gas temperature from 30 to 80 °C during 3 h. Inert gas injection will likely push the remained gas in cells, outside. The temperature of 65−80 °C is suitable for testing. The electrochemical reactions could be carried out at lower temperatures, such as 40−50 °C, but the reactions are less efficient and the fuel cell more likely to be flooded. The test which was considered for the PEM fuel cell was voltage-current test. It should be noticed that sudden changes in the current driven from the PEM fuel cell due to sudden changes in the load, cause the sticking together and closed spaces in C-Pt catalyst. To avoid this, it was planned to change the current with small steps (e.g. 1A) during the test. To calculate the required oxygen and hydrogen flow rate, Equations (3) and (4) are used [33]. The required O_2 and H_2 for the stack was calculated 0.1530 and 0.4615 SLPM (standard liter per minute) respectively.

$$\text{Oxygen consumption} = \frac{In}{4F} \ [\text{moles.s}^{-1}]$$
$$= \frac{32 \times 10^{-3} \times P_e}{4V_cF} = 8.29 \times 10^{-8} \times \frac{P_e}{V_c} \ [\text{kg.s}^{-1}] \quad (3)$$

$$\text{Hydrogen consumption} = \frac{In}{2F} \ [\text{moles.s}^{-1}]$$
$$= \frac{2.02 \times 10^{-3} \times P_e}{2V_cF} = 1.05 \times 10^{-8} \times \frac{P_e}{V_c} \ [\text{kg.s}^{-1}] \quad (4)$$

2.3 Data collection

Table 1 shows the set of test process conditions prepared for the fabricated PEM fuel cell.

Figure 3 shows the PEM fuel cell test stood in Material and research center of Isfahan.

Figure 4 shows the V-I test results. It was planned to change the current with small steps (e.g. 1A) during the test, to avoid catalyst adherence.

Table 1. Set of test process conditions.

Conditions \ Test numbers	Test 1	Test 2	Test 3	Test 4	Test 5	Test 6	Test 7
T (°C)	68	63	73	68	73	78	78
P (bar)	1	1.5	1	1.5	1.5	1	1

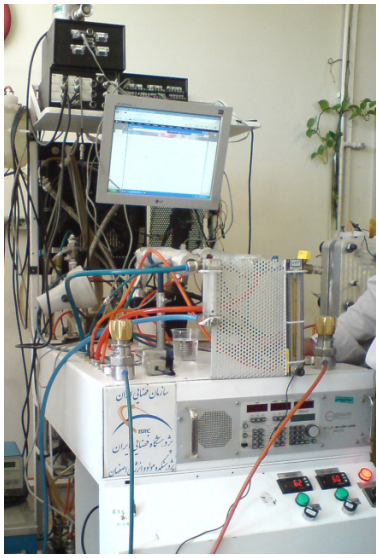

Fig. 3. Structure of the PEMFC test.

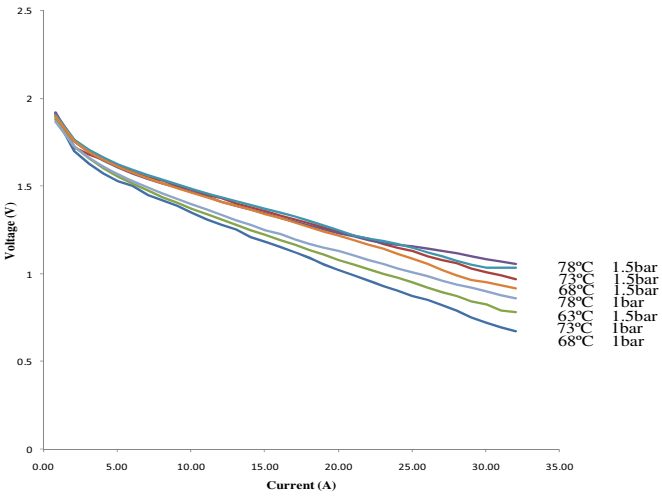

Fig. 4. V-I test results.

3 Parametric artificial neural networks

3.1 Parametric neural network

Artificial neural network is a powerful modeling tool that can be used to receive complex relations between input-output data. Many types of artificial neural network models have been developed that can be used for various applications. Essential component of the structure is simple. The weights can be changed or modified in various ways by the transfer function in order to define connections between the input layer, hidden layer and output layer. The built neural network can quickly receive and process the input data and deliver the outputs. Some of the notable features of artificial neural networks are:

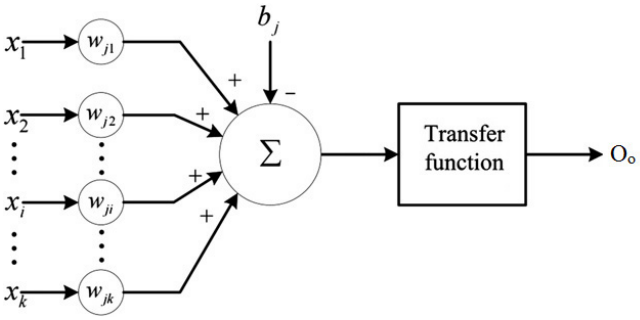

Fig. 5. Basic structure of neural networks.

- Adaptive learning.
- Self-organizing.
- Immediate operators.
- Fault tolerance.
- Grouping.
- Overall generalization.
- Stability-Flexibility [50].

The main advantage of neural network is the excellent nonlinear approximation ability, and there will be fewer assumptions for model construction compared to the traditional statistic models. The physical model is usually based on transfer phenomena, electrochemistry and heat conduction, however its derivation process is very complicated and its efficiency is not as well as the neural network model. Therefore, the neural network would be an appropriate choice for PEMFCs modeling. Figure 5 shows the basic structure of neural networks [51].

An input bias b_j in addition to input data is linked to the jth neuron. The output of the jth neuron will be:

$$O_o = F\left(\sum_{i=1}^{k} w_{ji}x_i - b_j\right) \tag{5}$$

In this study the presented neural network is a feed forward MPL structured network, with two hidden layers. The input layer consists of 3 neurons (for 3 input variables) and the output layer is a single neuron (for 1 output variable). Two hidden layers consist of 17 and 12 neurons, respectively. The ANN is trained by updating the weights using a back propagation learning rule. The error is returned from the intermediate and output layers and used to correct the weight coefficient. The output of the

last layer, compared with the desired value and the difference between them, generates an error. This error back to the previous layers is used as the weight updater. Moving backward, node input is multiplied to transfer functions derivate with respect to previous inputs, and the node output is created. This process continues until it reaches the first layer, and finally weight updating is completed by Equation (6). This process is continued until, for desired input, the network output will be close to the target.

$$w_{ji}(t+1) = w_{ji}(t) - \beta g(t) + \alpha\left(w_{ji}(t) - w_{ji}(t-1)\right) \tag{6}$$

$$g(t) = \frac{\partial(\mathrm{SSE})}{\partial w_{ji}}_{\;wji=wji(t)} \tag{7}$$

In which Sum of Square Error is defined as:

$$\mathrm{SSE} = \sum_{j=1}^{N} (t_j - O_j)^2 \tag{8}$$

The transfer function used in parametric neural network is a tangent hyperbolic one, since it is a bipolar function for upper and lower limits. Furthermore, back-propagation method needs differentiable function to adjust the weights. Equations (9) and (10) show the tangent hyperbolic transfer function and its derivative.

$$\tanh(x) = a = \frac{e^{x} - e^{-x}}{e^{x} + e^{-x}} \tag{9}$$

$$\tanh' x = (1 + \tanh x)(1 - \tanh x) \tag{10}$$

In this study "p" parameter has been defined in order to have a transfer function which can transform proportional due to network requirements. Changes of "p" parameter proportional to changes of the nonlinearity degree in the data-set would help network learning process. In other words, the "p" parameter makes the transfer function adaptive. Equation (11) shows the general form of the standard hyperbolic function.

$$f(x) = \frac{a\left(1 - e^{-\sigma x}\right)}{1 + e^{-\sigma x}} \tag{11}$$

This function can be controlled by a and σ parameters. Figure 6 illustrates the effect of these parameters on general form of the transfer function schematically.

To avoid drastic changes of a and σ a mathematical restrictive function can be utilized which is the logarithmic function. In other words, $\frac{1}{\mathrm{Ln}P}$ or e^{-P} can be used instead of a. p plays the role of regulator of the transfer function. This is possible by comparing the value of trained "p" with "1" if the parameter is near 1 then it is linear and the farther it is from 1 the more nonlinearity it has. Thus MPNN is somehow a gray box rather than a sole black box. Finally the transfer function used in the parametric neural network can be given by Equation (12) [52,53].

$$f_P(x) = \frac{1}{\ln(P)}\left(\tanh(\ln p \times x)\right) \tag{12}$$

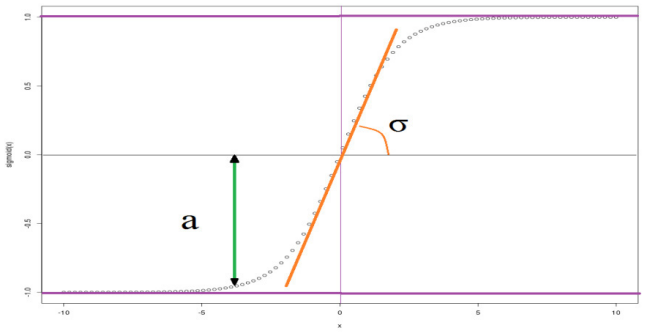

Fig. 6. Effect of a and σ parameters on general form of the transfer function.

Equation (13) presents the Mean Squares error function.

$$E = \frac{1}{2}\sum_{k}\left[t(k) - O_o(k)\right]^2 \tag{13}$$

Equations (14)–(20) present the change of "p" parameter and its relations:

$$p_{\mathrm{new}} = p_{\mathrm{old}} - \sigma\frac{\partial E}{\partial p_{\mathrm{old}}} \tag{14}$$

$$\delta_{o_o}(k) \equiv \frac{\partial E}{\partial O_o(k)} = O_o(k) - t(k) \tag{15}$$

$$\delta_{o_i}(k) \equiv \frac{\partial E}{\partial x_o(k)} = \frac{\partial E}{\partial O_o(k)}\frac{\partial O_o(k)}{\partial x_o(k)} = \partial_{o_o}(k) \times \tanh'(\ln p_k \times x_o(k)) \tag{16}$$

$$\delta_{h_o}(j) \equiv \frac{\partial E}{\partial O_h(j)} = \sum_{k}\frac{\partial E}{\partial x_o(k)} \cdot \frac{\partial x_o(k)}{\partial O_h(j)} = \sum_{k}\delta_{o_i} \times W_{k_j} \tag{17}$$

$$\delta_{h_i}(j) \equiv \frac{\partial E}{\partial x_h(j)} = \frac{\partial E}{\partial O_h(j)} \cdot \frac{\partial O_h(j)}{\partial x_h(j)} = \delta_{h_o}(j) \times \tanh'\left(\ln p_j \times x_h(j)\right) \tag{18}$$

$$\frac{\partial E}{\partial p_k} = \frac{\partial E}{\partial O_o(k)} \cdot \frac{\partial O_o(k)}{\partial p_k} = -\frac{1}{p_k \times \ln p_k} \times \left[\delta_{o_o}(k) \times O_o(k) - \delta_{o_i}(k) \times x_o(k)\right] \tag{19}$$

$$\frac{\partial E}{\partial p_j} = \frac{\partial E}{\partial h_o(k)} \cdot \frac{\partial h_o(j)}{\partial pj} = -\frac{1}{p_j \times \ln p_j} \times \left[\delta_{h_o}(j) \times O_h(j) - \delta_{h_i}(j) \times x_h(j)\right] \tag{20}$$

Figure 7 shows the structure of the designed parametric neural network.

Each data set was separated into two parts, namely training data and validation data. The training data were used to train the neural network to obtain the weights for the network and determine when training should be stopped. The training error will normally decrease during the initial phase of training. Training is done by assigning random weights to each neuron, evaluating the output of the network and calculating the error between the output of the network and the known results by means of an

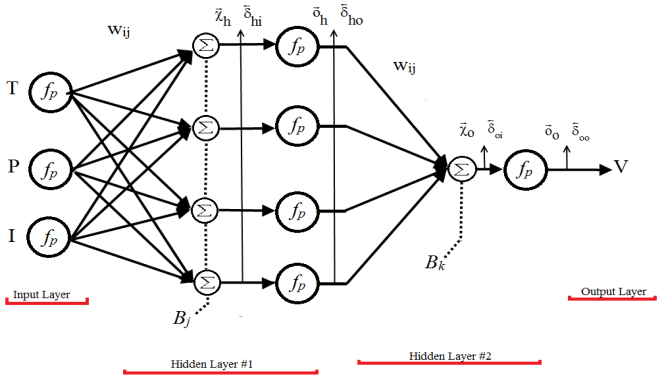

Fig. 7. Structure of the designed parametric neural network.

error or objective function. When the error becomes too large, the weights have to be adjusted and the process goes back for evaluate the output of the network. This cycle is repeated till the error becomes low or the convergence criterion is satisfied. However, when the network begins to over fit the data, the error on the training set will typically begin to rise. When the training error increases for a specified number of iterations, the training is stopped, and the weights and biases at the minimum of the training error are returned. The validation data were employed to assess the performance of a trained neural network with unseen data. 80% of the whole data were employed for the training part and the remaining data were used for the validation part. The training target was defined to continue the irritations for 6000 epochs.

After training the network one may look at the PNN and realize the degree of nonlinearity of the network. This is possible by comparing the value of trained "p" with "1". If the parameter is near to 1, then it is linear and the farer it is from 1 the more nonlinearity it has. Thus PNN is somehow a gray box rather than a sole black box.

3.2 Theoretical modeling of GMDH type of artificial neural network

The group method of data handling (GMDH) is a category of inductive algorithms for computer-based mathematical modeling of multi-parametric data sets that features parametric optimization of models. The method is a set of neurons in which various pairs of them in each layer are connected through a quadratic polynomial, therefore, generate new neurons in the next layer. This turn of phrase may be used in modeling to map inputs to outputs. This description includes the function $\hat{f}$ in order to predict the output $\hat{y}$ for a specified input vector $X = (x_1, x_2, x_3, \ldots, x_n)$. The function f and y are the actual input and output which are defined as followings:

$$y_i = f(x_{i1}, x_{i2}, x_{i3}, ..., x_{in}) \quad (i = 1, 2, 3, \ldots, M) \tag{21}$$

$$\hat{y}_i = \hat{f}(x_{i1}, x_{i2}, x_{i3}, ..., x_{in}) \quad (i = 1, 2, 3, \ldots, M) \tag{22}$$

Then, a GMDH type neural network must be applied in order to minimize the square of difference between the actual output and the predicted one:

$$\sum_{i=1}^{M} \left[\hat{f}(x_{i1}, x_{i2}, x_{i3}, ..., x_{in}) - \hat{y}_i\right]^2 \to \min \tag{23}$$

The connection between the input and output variables can be stated by a Kolmogorov-Gabor polynomial [38, 40–42]:

$$y = a_o + \sum_{i=1}^{n} a_i x_i + \sum_{i=1}^{n}\sum_{j=1}^{n} a_{ij} x_i x_j + \sum_{i=1}^{n}\sum_{j=1}^{n}\sum_{k=1}^{n} a_{ijk} x_i x_j x_k + \ldots \tag{24}$$

$$\hat{y} = G(x_i, x_j) = a_o + a_1 x_i + a_2 x_j + a_3 x_i^2 + a_4 x_j^2 + a_5 x_i x_j \tag{25}$$

For each pair of x_i, x_j as input variables, the coefficients a_i in Equation (25) are calculated by regression techniques, in order to minimize the difference between the actual output, y, and the calculated one, $\hat{y}$. In fact, a hierarchy of polynomials is built using the quadratic form provided in Equation (25) whose coefficients are calculated in a least-squares sense. In this respect, the coefficients of each quadratic function G_i are obtained to optimally fit the output in the whole set of input–output data pair, as follows:

$$E = \frac{\sum_{i}^{M} (y_i - G_i)^2}{M} \to \min \tag{26}$$

In order to construct the regression polynomial in the form of Equation (25) that best fits the dependent observations $(y_i, i = 1, 2, \ldots, M)$ in a least-squares sense, in the GMDH algorithm, all the possibilities of two independent variables out of total n input variables are selected. In fact, $\binom{n}{2} = \frac{n(n-1)}{2}$ neurons will be consequently built up in the first hidden layer of the feed forward network from the observations $\{(y_i, x_{ip}, x_{iq}); (i = 1, 2, \ldots, M\}$ for different $p, q\hat{I}\{1, 2, \ldots, n\}$. The M data triples $\{(y_i, x_{ip}, x_{iq}); (i = 1, 2, \ldots, M\}$ could be built from the observation utilizing such $p, q\hat{I}\{1, 2, \ldots, n\}$ in the form of

$$\begin{bmatrix} x_{1p} & x_{1q} & y_1 \\ x_{2p} & x_{2q} & y_2 \\ x_{3p} & x_{3q} & y_M \end{bmatrix}$$

Using the quadratic sub-expression in the form of Equation (25) for each row of M data triples, the following matrix equation can be readily obtained as

$$Aa = Y \tag{27}$$

$$a = \{a_0, a_1, a_2, a_3, a_4, a_5\} \tag{28}$$

$$Y = \{y_1, y_2, y_3, \ldots y_M\}^T \tag{29}$$

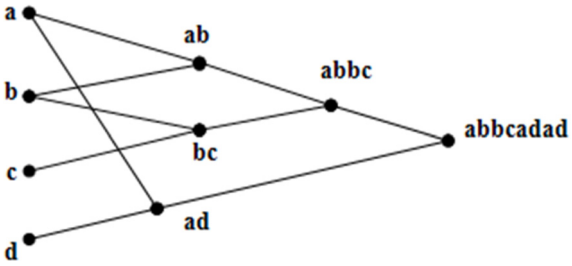

Fig. 8. A generalized GMDH network structure of chromosome.

where a is the vector of unknown coefficients for the quadratic polynomial in Equation (25), and Y is the vector of output values from observation. A is given by:

$$A = \begin{bmatrix} 1 & x_{1p} & x_{1q} & x_{1p}x_{1q} & x_{1p}^2 & x_{1q}^2 \\ 1 & x_{2p} & x_{2q} & x_{2p}x_{2q} & x_{2p}^2 & x_{2q}^2 \\ -- & -- & -- & -- & -- & -- \\ 1 & x_{Mp} & x_{Mq} & x_{Mp}x_{Mq} & x_{Mp}^2 & x_{Mq}^2 \end{bmatrix} \tag{30}$$

The least-squares technique from multiple-regression result is expressed as:

$$a = \left(A^T A\right)^{-1} A^T \tag{31}$$

This process for each neuron of the next hidden layer is iterated and neurons in each layer are only connected to the neuron in its adjoining layer. Such a solution from normal equations is directly rather susceptible to round off errors [48,49,54–57]. Taking this advantage, it was possible to perform a simple encoding scheme for the genotype of each character in the population as already proposed by [46–49]. The encoding schemes are shown in Figure 8.

According to Figure 8, output neuron (abbcadad) includes twice ad because the neuron (ad) at the first layer is connected to the output layer by directly going through the second layer. This process takes place when a neuron passes some adjoining hidden layers and connects to another neuron in the next following hidden layer. In this method, the number of repetitions of neuron was given by $2^{\tilde{n}}$ where $\tilde{n}$ is the number of the passed hidden layers [46–49].

For the validity check three parameters are used: R^2 as the absolute fraction of variance, RMSE as the root-mean squared error and MAPE as the mean absolute percentage of error, which are given by:

$$R^2 = 1 - \left[\frac{\sum_{i=0}^{M}\left(Y_{i(\text{model})} - Y_{i(\text{Actual})}\right)^2}{\sum_{i=1}^{M}\left(Y_{i(\text{Actual})}\right)^2}\right] \tag{32}$$

$$\text{RMSE} = \left[\frac{\sum_{i=0}^{M}\left(Y_{i(\text{model})} - Y_{i(\text{Actual})}\right)^2}{M}\right]^{1/2} \tag{33}$$

$$\text{MAPE} = \left[\frac{\sum_{i=0}^{M}\left|Y_{i(\text{model})} - Y_{i(\text{Actual})}\right|}{M\sum_{i=1}^{M}\left(Y_{i(\text{Actual})}\right)}\right] \tag{34}$$

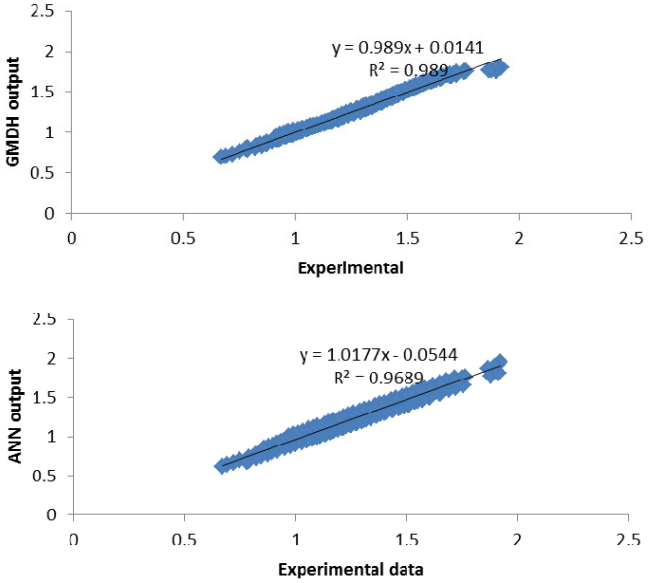

Fig. 9. R^2 for: (a) GMDH model and (b) ANN model.

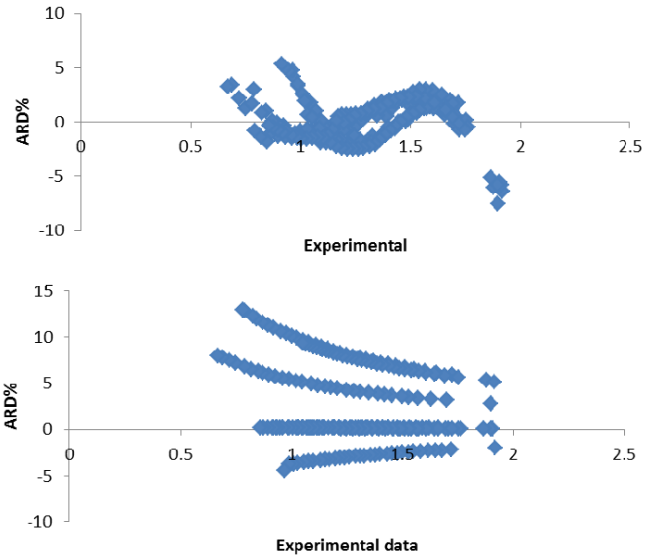

Fig. 10. Variation of relative error against corresponding experimental voltage values (a) for GMDH model; (b) for ANN model.

4 Results and discussions

Figure 9 depicts a comparison between ANN output and GMDH output, while Figures 9a and 9b are for ANN and GMD respectively. As can be seen, both ANN and GMDH, have trained networks very well. Trained GMDH model according to slightly higher R^2 is reasonable model.

In Figure 10, the deviation percentage of the GMDH and ANN trained networks output data, from experimental data is shown. Figure 10a shows the trained network by ANN with maximum deviation of 14% and Figure 10b shows the trained network by GMDH where the maximum deviation is 8%.

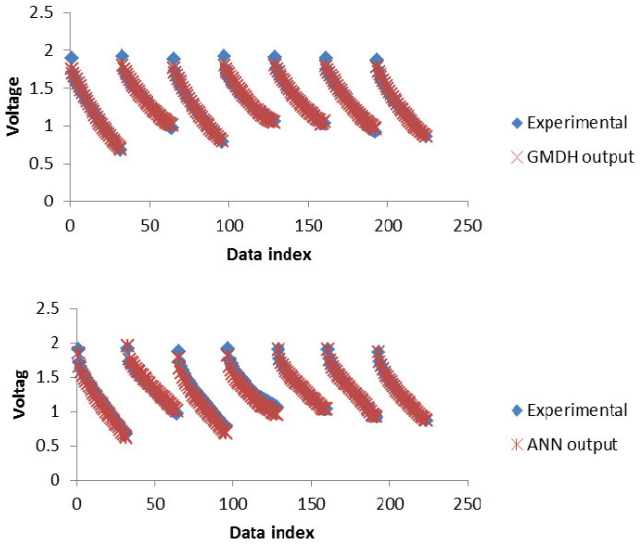

Fig. 11. Comparison between measured and predicted voltage: (a) for GMDH and (b) for ANN.

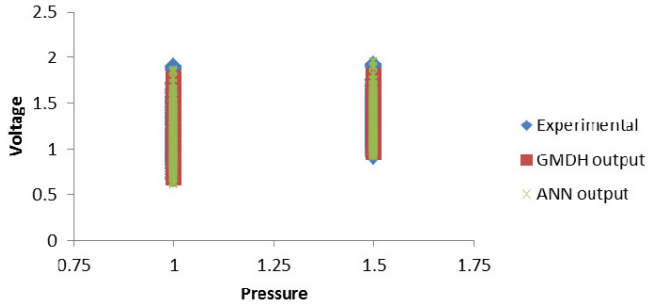

Fig. 12. Comparison between experimental voltage and outcomes of the ANN and GMDH approaches versus pressure.

In Figure 11, the agreement between the ANN and GMDH outputs with experimental results is compared, where Figures 11a and 11b are for ANN and GMDH respectively. The agreement with experimental results is high in both networks, but GMDH results are still slightly better.

Figure 12 shows the changes in voltage among changes of pressure for the experimental results and the results of ANN and GMDH. As it is shown there is a very good agreement between the results of these models and experimental results.

In Figure 13 the voltage changes among changes of current for the experimental results and the results of ANN and GMDH are shown. As it is shown, in higher temperature and pressure fuel cell achieve higher values of power.

Temperature changes among voltage changes for the experimental results and the results of ANN and GMDH are shown in Figure 14. As it is shown there is a very good agreement between the results of these models and experimental results and deviations are negligible.

One feature of GMDH method is that in this method for each output by weighting of each input an equation can be produced. This method defines the best weight

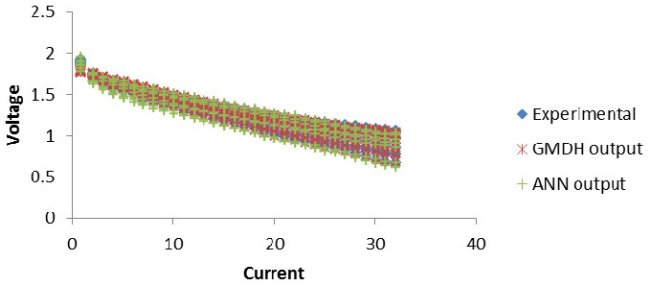

Fig. 13. Comparison between experimental voltage and outcomes of the ANN and GMDH approaches versus current.

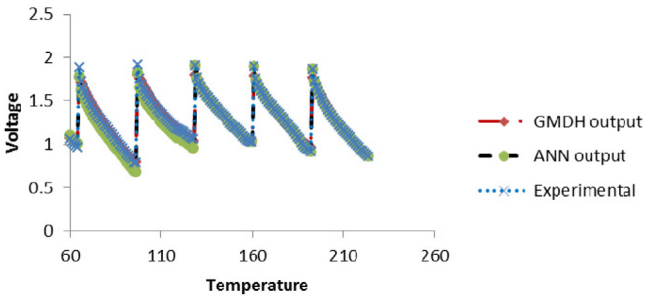

Fig. 14. Comparison between experimental voltage and outcomes of the ANN and GMDH approaches versus temperature.

Table 2. Comparison between the performances of GMDH and ANN model.

	GMDH model	ANN model
R^2	0.98900000000	0.9689000000
MAPE	0.00006982917	0.0001481063
RMSE	0.02851850400	0.0590257550

for each set of inputs and therefore produces the best formulas with the highest accuracy. The equation is as follows:

$$V = 0.00144548 + N12 \times 1.16105 - N24 \times 0.162184 \quad (35)$$

$$N12 = 1.68554 - I \times 0.103175 + I \times N34 \times 0.0483137 + (I)^2 \times 0.00041073 + N34^2 \times 0.0796619$$

$$N24 = -7.10333 + N27 \times 1.44962 - N27 \times N34 \times 0.359465 + N34 \times 10.7265 - N34^2 \times 4.02303$$

$$N27 = 1.53042 + P \times 0.396269 + P \times I \times 0.0119142 - (P)^2 \times 0.130447 - I \times 0.0566935 + (I)^2 \times 0.000410735$$

$$N34 = -2.60027 + T \times 0.100025 - T \times P \times 0.0248346 - (T)^2 \times 0.000455714 - P \times 0.136567 + (P)^2 \times 0.886792$$

Some statistical measures for voltage are given in Table 2, respectively. The correlation coefficient is high in all sections and this shows that accuracy of the trained networks is appreciated.

5 Conclusions and perspectives

In this study, experimental results were obtained from the PEM-type fuel cell which has been manufactured and tested in laboratory. By employing these experimental results in ANN and GMDH algorithms, two models were designed and the results of these two models have been compared. Parametric neural network has a "p" parameter in its tangent hyperbolic transfer function which makes it adaptive due to different nonlinearity degrees of network input data. The PNN model can realize the degree of nonlinearity of the input data. Thus, PNN is somehow a gray box rather than a sole black box. By utilizing GMDH algorithm we could also define high accurate equations for output voltage depending on input temperature, pressure and gas flow for training networks. Both methods showed an excellent agreement with experimental data while the GMDH model had less deviation. For the first time, to model and predict the fuel cell voltage GMDH algorithm was employed in this work. The results of the networks trained by ANN and GMDH are very reasonable and they can be used in the design of a PEM fuel cell.

References

[1] S.J. Peighambardoust, S. Rowshanzamir, M. Amjadi, Review of the proton exchange membranes for fuel cell applications, Int. J. Hydrogen Energy 35 (2010) 9349–9384

[2] M. Radulescu, V. Ayel, O. Lottin, M. Feidt, B. Antoine, C. Moyne, D. Le Noc, S. Le Doze, Natural gas electric generator powered by polymer exchange membrane fuel cell: Numerical model and experimental results, Energy Convers. Manage. 49 (2008) 326–335

[3] O. Erdinc, M. Uzunoglu, Recent trends in PEM fuel cell-powered hybrid systems: Investigation of application areas, design architectures and energy management approaches, Renew. Sustain. Energy Rev. 14 (2010) 2874–2884

[4] O.S. Suslu, I. Becerik, On-Board Fuel Processing for a Fuel Cell-Heat Engine Hybrid System, Energy and Fuels 23 (2009) 1858–1873

[5] M. Hu, A. Gu, M. Wang, X. Zhu, L. Yu, Three dimensional, two phase flow mathematical model for PEM fuel cell. Part I. Model development, Energy Convers. Manage. 45 (2004) 1861–1882

[6] M. Hu, A. Gu, M. Wang, X. Zhu, L. Yu, Three dimensional, two phase flow mathematical model for PEM fuel cell. Part II. Analysis and discussion of the internal transport mechanisms, Energy Convers. Manage. 45 (2004) 1883–1916

[7] G. Hu, J. Fan, A Three-Dimensional, Multicomponent, Two-Phase Model for a Proton Exchange Membrane Fuel Cell with Straight Channels, Energy and Fuels 20 (2006) 738–747

[8] A.R.M. Sadiq Al-Baghdadi, H.A.K. Shahad Al-Janabi, Influence of the Design Parameters in a Proton Exchange Membrane (PEM) Fuel Cell on the Mechanical Behavior of the Polymer Membrane, Energy and Fuels 21 (2007) 2258–2267

[9] M. De Falco, Ethanol membrane reformer and PEMFC system for automotive application, Fuel 90 (2011) 739–747

[10] X.-D. Wang, W.-M. Yan, Y.-Y. Duan, F.-B. Weng, G.-B. Jung, C.-Y. Lee, Numerical study on channel size effect for proton exchange membrane fuel cell with serpentine flow field, Energy Convers. Manage. 51 (2010) 959–968

[11] M. Uzunoglu, M.S. Alam, Dynamic modeling, design and simulation of a PEM fuel cell/ultra-capacitor hybrid system for vehicular applications, Energy Convers. Manage. 48 (2007) 1544–1553

[12] P. Corbo, F.E. Corcione, F. Migliardini, O. Veneri, Energy management in fuel cell power trains, Energy Convers. Manage. 47 (2006) 3255–3271

[13] R.N. Methekar, V. Prasad, R.D. Gudi, Dynamic analysis and linear control strategies for proton exchange membrane fuel cell using a distributed parameter model, Power Sources 165 (2007) 152–170

[14] J.J. Baschuk, Li. Xianguo, Modeling of polymer electrolyte membrane fuel cells with variable degrees of water flooding, Power Sources 86 (2000) 181–196

[15] T.V. Nguyen, R.E. White, A Water and Heat Management Model for Proton-Exchange, J. Electrochem. Soc. 140 (1993) 2178–2186

[16] T.F. Fuller, J. Newman, Water and Thermal Management in Solid-Polymer-Electrolyte Fuel cell, J. Electrochem. Soc. 140 (1993) 1218–1225

[17] D.M. Bernardi, M.W. Verbrugge, A mathematical model of the solid-polymer-electrolyte fuel cell, J. Electrochem. Soc. 139 (1992) 2477–2491

[18] Z.H. Wang, C.Y. Wang, K.S. Chen, Two-phase flow and transport in the air cathode of proton exchange membrane fuel cells, J. Power Sources 94 (2001) 40–50

[19] C.Y. Du, P.F. Shi, J. Harbin, Multi-input and multi-output neural model of the mechanical nonlinear behavior of a PEM fuel cell system, Inst. Technol. 38 (2006) 1511–1514

[20] R.P. Pathapati, X. Xue, J. Tang, A new dynamic model for predicting transient phenomena in a PEM fuel cell system, Renewable Energy 30 (2005) 1–22

[21] F. Mueller, J. Brouwer, S. Kang, H. Kim, K. Min, Quasi-three dimensional dynamic model of a proton exchange membrane fuel cell for system and controls development, J. Power Sources 163 (2007) 814–829

[22] Y. Shan, S.Y. Choe, A high dynamic PEM fuel cell model with temperature effects, J. Power Sources 145 (2005) 30–39

[23] W. Na, B. Gou, B. Diong, Nonlinear control of PEM fuel cells by exact linearization, Proc. IEEE Ind. Appl. Conf. 4 (2005) 2937–2943

[24] A. Nasiri, V.S. Rimmalapudi, A. Emadi, D.J. Chmielewski, S. Al-Hallaj, Active control of a hybrid fuel cell-battery system, Power Electronics and Motion Control Conference, 2004

[25] D.E. Adams, R.J. Randall, Neural model of the dynamic behaviour of a non-linear mechanical system, Proceedings of the 23rd International Conference on Noise and Vibration Engineering ISMA, 1998, pp. 517–529

[26] S.O.T. Ogaji, R. Singh, P. Pilidis, M. Diacakis, Modeling fuel cell performance using artificial intelligence, J. Power Sources 154 (2006) 192–197

[27] S. Ou, L.E.K. Achenie, A hybrid neural network model for PEM fuel cells, J. Power Sources 140 (2005) 319–330
[28] A.U. Chávez-Ramírez, R. Muñoz-Guerrero, S.M. Durón-Torres, M. Ferraro, G. Brunaccini, F. Sergi, V. Antonucci, High power fuel cell simulator based on artificial neural network, Int. J. Hydrogen Energy 35 (2010) 12125–12133
[29] N.S. Sisworahardjo, T. Yalcinoz, Neural network model of 100 W portable PEM fuel cell and experimental verification, Int. J. Hydrogen Energy 35 (2010) 9104–9109
[30] K.Y. Chang, The optimal design for PEMFC modeling based on Taguchi method and genetic algorithm neural networks, Int. J. Hydrogen Energy 36 (2011) 13683–13694
[31] D. Paclisan, W. Charon, Real time modeling of the dynamic mechanical behaviour of PEMFC thanks to neural networks, Eng. Appl. Artif. Intell. 26 (2013) 706–713
[32] J. Kim, I. Lee, State-of-health diagnosis based on hamming neural network using output voltage pattern recognition for a PEM fuel cell, Int. J. Hydrogen Energy 37 (2012) 4280–4289
[33] E. Sanchez, T. Shibata, L.A. Zadeh, Genetic algorithms and fuzzy logic systems, World Scientific, River edge NJ, 1997
[34] K. Kristinson, G. Dumont, System identification and control using genetic algorithms, J. IEEE Trans. Syst. Man Cybern 22 (1992) 1033–1046
[35] T. Somayeh, M.H. Ahmadi, A. Kasaeian, A.H. Mohammadi, Artificial neural network, ANN-PSO and ANN-ICA for modelling the Stirling engine. International Journal of Ambient Energy ahead-of-print (2014) 1-13, DOI:10.1080/01430750.2014.986289
[36] M.H. Ahmadi, M. Mehrpooya, N. Khalilpoor, Artificial neural networks modelling of the performance parameters of the Stirling engine. International Journal of Ambient Energy ahead-of-print (2014) 1-7, DOI:10.1080/01430750.2014.964370
[37] M.H. Ahmadi, S. Sorouri Ghare Aghaj, A. Nazeri, Prediction of power in solar stirling heat engine by using neural network based on hybrid genetic algorithm and particle swarm optimization. Neural Computing and Applications 22 (2013) 1141–1150
[38] A.G. Ivakhnenko, Polynomial Theory of Complex Systems, IEEE Trans. Syst. Man Cybern SMC-1 (1971) 364–378
[39] S.J. Farlow Self-organizing method in modelling: GMDH type algorithm, Marcel Dekker Inc, 1984
[40] J.A. Mueller, F. Lemke, Self-organizing data mining: an intelligent approach to extract knowledge from data, Pub. Libri, Hamburg, 2000
[41] M.H. Ahmadi, M.A. Ahmadi, M. Mehrpooya, M.A. Rosen, Using GMDH Neural Networks to Model the Power and Torque of a Stirling Engine. Sustainability 7 (2015) 2243–2255
[42] C.M. Fonseca, P.J. Fleming, Nonlinear system identification with multi-objective genetic algorithm, Proceedings of the 13th World congress of the international federation of automatic control, San Francisco, Pergamon Press, California, 1996, pp. 187–192
[43] G.P. Liu, V. Kadirkamanathan, Multi-objective criteria for neural networkstructure selection and identification of nonlinear systems using genetic algorithms, IEEE Proc. Control Theory Appl. 146 (1999) 373–382
[44] N. Nariman-Zadeh, A. Darvizeh, R. Ahmad-Zadeh, Hybrid Genetic Design of GMDH-Type Neural Networks Using Singular Value Decomposition for Modelling and Prediction of the Explosive Cutting Process, J. Eng. Manufact. 217 (2003) 779–790
[45] V.W. Porto, Evolutionary computation approaches to solving problems in neural computation. In: T. Back, D.B. Fogel, Z. Michalewicz (eds.), Handbook of evolutionary computation, Institute of Physics Publishing and Oxford University Press, New York, 1997, pp. 1–6
[46] X. Yao, Evolving artificial neural networks, Proc. IEEE 87 (1999) 1423–1447
[47] E.F. Vasechkina, V.D. Yarin, Evolving polynomial neural network by means of genetic algorithm: some application examples, 2001, Complex Int 9
[48] X. Yao, Evolving Artificial Neural Networks, Proc. IEEE 87 (1999) 1423–1447
[49] N. Nariman-zadeh, K. Atashkari, A. Jamali, A. Pilechi, X. Yao, Inverse modelling of multi-objective thermodynamically optimized turbojet engines using GMDH-type neural networks and evolutionary algorithms, J. Eng. Optim. 37 (2005) 437–462
[50] S.S. Haykin, Neural Networks A Comprehensive Foundation, Prentice Hall, Upper Saddle River, NJ, 1999
[51] P.D. Wasserman, Neural computing theory and practice, Van Nostrand Reinhold, New York, 1989
[52] M. Hasheminejad, J. Murata, K. Hirasawa, System Identification Using Neural Networks with parametric Sigmoid Functions, Trans. Soc. Instrum. Control Eng. 31 (1995) 277–283
[53] M. Hasheminejad, J. Murata, K. Hirasawa, Control Design Using Parametric Neural Networks, Trans. Soc. Instrum. Control Eng., 1995
[54] K. Atashkari, N. Nariman-Zadeh, A. Jamali, A. Pilechi, Thermodynamic Pareto optimization of turbojet using multi-objective genetic algorithm, Int. J. Thermal Sci. 44 (2005) 1061–1071
[55] K. Atashkari, N. Nariman-Zadeh, M. Golcu, A. Khalkhali, A. Jamali, Modelling and multi-objective optimization of a variable valve-timing spark-ignition engine using polynomial neural networks and evolutionary algorithms, Energy Convers. Manage. 48 (2007) 1029–1041
[56] A. Jamali, N. Nariman-Zadeh, A. Darvizeh, A. Masoumi, S. Hamrang, Multi-objective evolutionary optimization of polynomial neural networks for modelling and prediction of explosive cutting process, Eng. Appl. Artif. Intell. 22 (2009) 676–687
[57] M.H. Ahmadi, M.A. Ahmadi, S.A. Sadatsakkak, M. Feidt, Connectionist intelligent model estimates output power and torque of stirling engine. Renewable and Sustainable Energy Reviews 50 (2015) 871–883